

WHAT CAN SNO NEUTRAL CURRENT RATE TEACH US ABOUT THE SOLAR NEUTRINO ANOMALY

ABHIJIT BANDYOPADHYAY, SANDHYA CHOUBEY, SRUBABATI GOSWAMI

*Saha Institute of Nuclear Physics
Bidhannagar, Kolkata 700 064, India*

D.P.ROY

*Tata Institute of Fundamental Research
Homi Bhabha Road, Mumbai 400 005, India*

We investigate how the anticipated neutral current rate from *SNO* will sharpen our understanding of the solar neutrino anomaly. Quantitative analyses are performed with representative values of this rate in the expected range of 0.8 – 1.2. This would provide a 5 – 10 σ signal for ν_e transition into a state containing an active neutrino component. Assuming this state to be purely active one can estimate both the 8B neutrino flux and the ν_e survival probability to a much higher precision than currently possible. Finally the measured value of the *NC* rate will have profound implications for the mass and mixing parameters of the solar neutrino oscillation solution.

Keywords: massive neutrino, mixing, solar neutrinos

PACS NO(s): 14.60.pq,14.60.Lm,13.15.+g

A large number of experiments have observed anomalously low solar neutrino flux ^{1,2,3,4} compared to the standard solar model (SSM) prediction ⁵. They are the radiochemical experiments on *Ga* ¹ and *Cl* ² targets as well as the water Cerenkov experiments from Super Kamiokande (SK) ³ and Sudbury Neutrino Observatory (*SNO*) ⁴. SK observes the emitted electron from elastic scattering

$$\nu + e \rightarrow \nu + e, \quad (1)$$

while *SNO* observes it from the charged current process

$$\nu_e + d \rightarrow p + p + e \quad (2)$$

using a heavy water target. Both the experiments probe the high energy tail of the solar neutrino spectrum, which is dominated by the 8B neutrino flux. The SK elastic scattering process (1) is sensitive to ν_e via CC and *NC* interactions; but it also has a limited sensitivity to $\nu_{\mu,\tau}$ via the *NC* interaction. On the other hand the

SNO experiment is looking separately at the *NC* rate, which has equal sensitivity to all the active neutrino flavors, via

$$\nu + d \rightarrow \nu + p + n, \quad (3)$$

followed by the neutron capture by *NaCl*. The resulting excited state decays via γ emission, which constitutes the *NC* signal. The *SNO* experiment is expected to report its first *NC* rate shortly, corresponding to a data sample of $\sim 10^3$ events – i.e. similar statistical accuracy as their 1st CC data.⁴ The purpose of our work is to critically analyse how far this data will enhance our understanding of the solar neutrino anomaly and its solution.

By far the most plausible solution of the solar neutrino anomaly is in terms of neutrino oscillation, and in particular the oscillation of ν_e into another active flavor ν_a , which can be any combination of ν_μ and ν_τ . Indeed we have made considerable progress in understanding the solar neutrino anomaly and its oscillation solution over the past few months by combining the CC rate from *SNO* with the SK elastic scattering data^{6,7,8,9,10}. Firstly they disfavour ν_e transition into a sterile neutrino ν_s at the 3σ level in a model independent way.⁴ Secondly, assuming only transition between ν_e and ν_a , one can estimate both the 8B flux and the ν_e survival probability, although with fairly large uncertainties.⁷ Thirdly one can do a combined analysis of the *SNO*, *SK* and the earlier radiochemical data assuming SSM and the $\nu_e \rightarrow \nu_a$ oscillation model.^{7,8,9} One sees that the result has narrowed down to only two possible solutions, both having large mixing angles – i.e. the so called LMA and LOW solutions. We shall see below that each of the above results can be significantly sharpened further by including the *NC* rate from *SNO*.

Table 1. The observed solar neutrino rates relative to the *SSM* predictions are shown along with their compositions and threshold energies for different experiments. For the *SK* experiment the ν_e contribution to the rate R is shown in parentheses assuming $\nu_e \rightarrow \nu_a$ transition.

experiment	R	composition	E_{th} (Mev)
<i>Ga</i>	0.584 ± 0.039	<i>pp</i> (55%), <i>Be</i> (25%), <i>B</i> (10%)	0.2
<i>Cl</i>	0.335 ± 0.029	<i>B</i> (75%), <i>Be</i> (15%)	0.8
<i>SK</i>	0.459 ± 0.017 (0.351 ± 0.017)	<i>B</i> (100%)	5.0
<i>SNO(CC)</i>	0.347 ± 0.027	<i>B</i> (100%)	7.0

Table 1 lists the observed solar neutrino rates of the *Ga*, *Cl*, *SK* and *SNO (CC)* experiments relative to the corresponding *SSM* predictions. The compositions of the respective solar neutrino fluxes are also indicated along with the threshold

energies. Assuming the SSM neutrino fluxes and the transition of ν_e into an active flavor ν_a one can write the SK elastic scattering rate relative to the SSM prediction in terms the survival probability, i.e.

$$R_{SK}^{el} = P_{ee} + rP_{ea} = P_{ee} + r(1 - P_{ee}), \quad (4)$$

where $r = \sigma_{\nu_a}^{NC} / \sigma_{\nu_e}^{CC+NC} \simeq 0.17$ is the ratio of $\nu_{\mu,\tau}$ to ν_e elastic scattering cross-sections (1).⁶ The resulting value of the ν_e survival probability P_{ee} is shown parenthetically in Table 1. The other rates shown in this table are identical to the corresponding P_{ee} , since they are sensitive to ν_e only.

As we see from table 1, the *SK* and *SNO* experiments are sensitive only to the 8B neutrino spectrum. While the shape of this spectrum is predicted with good precision by the SSM, there is a large uncertainty in the predicted normalisation,⁵

$$\phi_B = 5.05 \times 10^6 (1_{-0.16}^{+0.20}) \text{ cm}^{-2} \text{ s}^{-1}, \quad (5)$$

arising from the uncertainty in the ${}^7Be + p \rightarrow {}^8B + \gamma$ cross-section. Therefore we shall introduce a constant parameter f_B to denote the normalisation of the 8B neutrino flux relative to the SSM prediction. Then the SK elastic scattering and the *SNO CC* and *NC* scattering rates relative to the corresponding *SSM* predictions are

$$R_{SK}^{el} = f_B P_{ee} + f_B r P_{ea}, \quad (6)$$

$$R_{SNO}^{CC} = f_B P_{ee}, \quad (7)$$

$$R_{SNO}^{NC} = f_B (P_{ee} + P_{ea}), \quad (8)$$

which hold for the general case of ν_e transition into any combination of ν_a and ν_s . It should be noted here that these three measurements do not have identical energy ranges. The *SK* and *SNO CC* data start from neutrino energies of 5 and 7 MeV respectively, while the response function of the *SNO NC* measurement extends marginally below 5 MeV. However the SK rate and the resulting survival probability show energy independence down to 5 MeV to a very good precision. The *SNO CC* rate shows energy independence as well, although to lesser precision. Therefore it is reasonable to assume a common survival probability for all the three measurements.

As recently discussed in,⁶ the SK elastic and the *SNO CC* rates can be combined to access information on *NC* scattering, so that in principle there is no new information contained in the *SNO NC* rate. In fact eqs. (6,7,8) can be seen to give the sum rule

$$R_{SNO}^{NC} = R_{SNO}^{CC} + (R_{SK}^{el} - R_{SNO}^{CC})/r, \quad (9)$$

which predicts $R_{SNO}^{NC} = 1.0 \pm 0.24$.⁶ However the large uncertainty in this prediction reflects the low sensitivity of R_{SK}^{el} to *NC* scattering, which is weighted by a small co-efficient r . On the other hand the expected *NC* scattering rate from *SNO* at the

level of $\sim 10^3$ events should have a similar precision as their present CC rate, i.e. $\pm 8\%$, which will ultimately go up to $\pm 5\%$. Keeping in mind the predicted range of R_{SNO}^{NC} we shall assume

$$R_{SNO}^{NC} = 1.0 \pm .08, 1.2 \pm .08, 0.8 \pm .08 \quad (10)$$

as three representative values of the NC scattering rate expected from SNO and analyse the implications for the solar neutrino anomaly. We shall see below that the R_{SNO}^{NC} input will lead to qualitative improvement in the results of all the three types of analyses mentioned earlier.

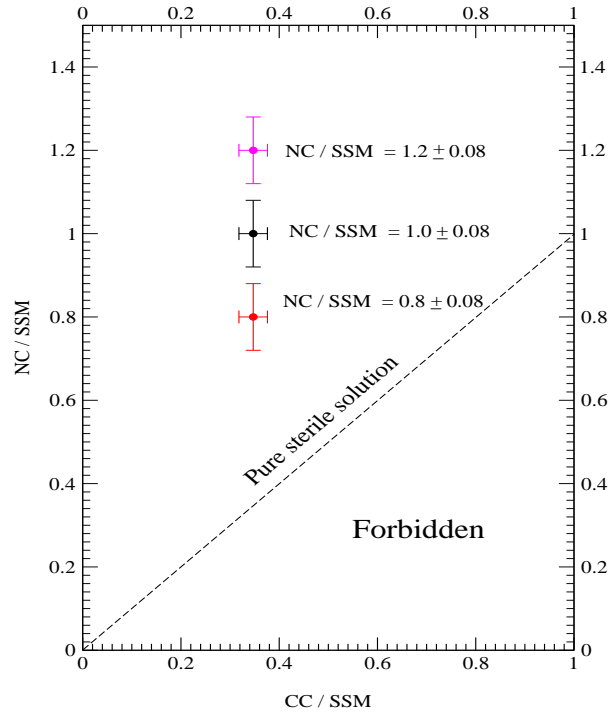


Fig. 1. The SNO CC and NC rates shown relative to their SSM predictions for the three representative values of the latter. The dashed line is the prediction of the pure ν_e to ν_s transition

General Analysis of $\nu_e \rightarrow \nu_{a,s}$ Transitions: Let us start with a model independent analysis of ν_e transition into an active neutrino flavour ν_a . One sees from eqs.

(6,7) that the observed excess of R_{SK}^{el} over the R_{SNO}^{CC} in Table 1 constitutes a 3σ signal for $\nu_e \rightarrow \nu_a$ transition or equivalently a 3σ signal against a pure $\nu_e \rightarrow \nu_s$ transition.⁴ Similarly an observed excess of R_{SNO}^{NC} (8) over R_{SNO}^{CC} (7) will constitute a model independent signal for the $\nu_e \rightarrow \nu_a$ transition P_{ea} . Fig. 1 compares the R_{SNO}^{NC} values of eq. (10) with the current value of R_{SNO}^{CC} . It shows that an observed value of R_{SNO}^{NC} in the range of $0.8 - 1.2(\pm 0.08)$ will constitute of $5 - 10 \sigma$ signal for $\nu_e \rightarrow \nu_a$ transition i.e. transition of ν_e into a state of atleast partly active neutrino.

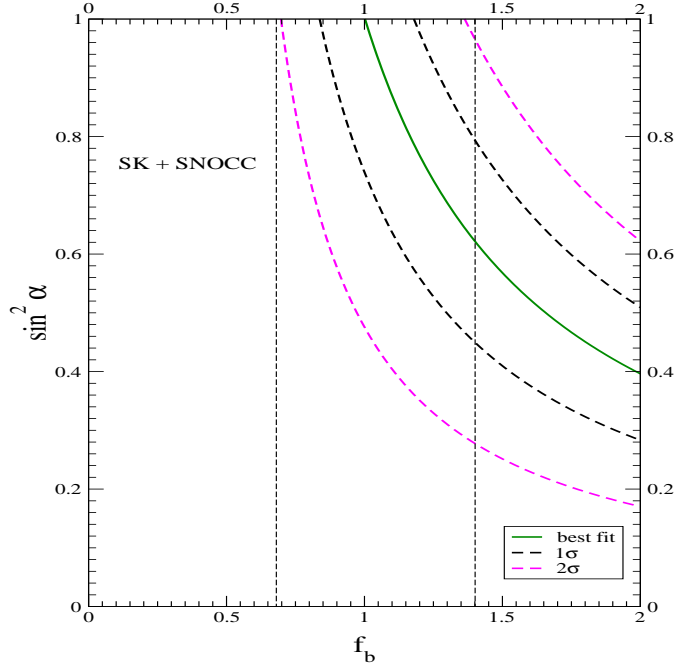


Fig. 2. Best fit value of the 8B neutrino flux shown along with the 1σ and 2σ limits against the model parameter $\sin^2 \alpha$, representing ν_e transition into a mixed state ($\nu_a \sin \alpha + \nu_s \cos \alpha$). The dashed line denote the $\pm 2\sigma$ limits of the SSM .

Unfortunately one cannot get a model independent estimate of the $\nu_e \rightarrow \nu_a$ transition probability P_{ea} , since the above excess corresponds to the product $f_B P_{ea}$. In fact it is evident from eqs. (6-8) that these two quantities can not be separated with or without the P_{SNO}^{NC} input. In other words for the general case of ν_e transition into a mixture of active and sterile neutrinos,

$$\nu_a \sin \alpha + \nu_s \cos \alpha, \quad (11)$$

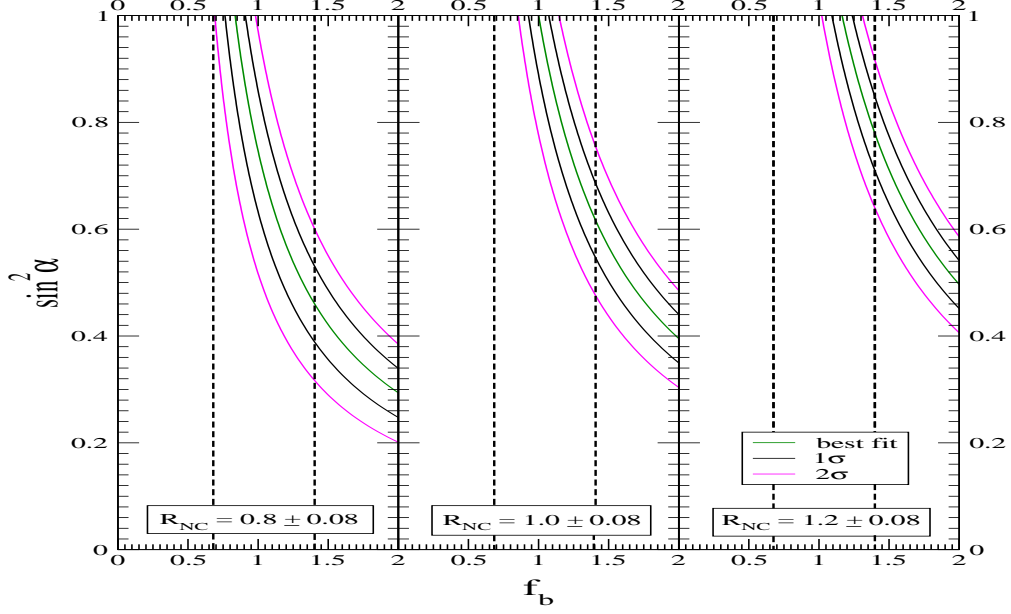


Fig. 3. Same as Fig. 2 but including the NC rate to the fit along with the SK elastic and SNO CC rates. The dashed lines denote the $\pm 2\sigma$ limits of the SSM .

one can rewrite eqs. (6) and (8) as

$$R_{SK}^{el} = f_B P_{ee} + f_B r \sin^2 \alpha (1 - P_{ee}), \quad (12)$$

$$R_{SNO}^{NC} = f_B P_{ee} + f_B \sin^2 \alpha (1 - P_{ee}). \quad (13)$$

Then it will not be possible to separately estimate the parameters f_B and $\sin^2 \alpha$. One can only determine the following combination in two different ways, i.e.

$$\sin^2 \alpha (f_B - R_{SNO}^{CC}) = (R_{SK}^{el} - R_{SNO}^{CC})/r, \quad (14)$$

$$\sin^2 \alpha (f_B - R_{SNO}^{CC}) = R_{SNO}^{NC} - R_{SNO}^{CC}. \quad (15)$$

A two parameter fit to (14) was done in ref.⁶ to determine the allowed contour in the $f_B - \sin^2 \alpha$ plane. We shall instead treat $\sin^2 \alpha$ as a model parameter. And for each input value of $\sin^2 \alpha$ we shall determine f_B first from eq. (14) and then from a weighted average of eqs. (14) and (15). The results are shown as lines corresponding to the central value of f_B along with the 1σ and 2σ boundaries in

the $f_B - \sin^2 \alpha$ plane in Figs. 2 and 3. The advantage of this procedure is that for $\sin^2 \alpha = 1$ the 1σ and 2σ ranges of f_B shown correspond to those of the pure $\nu_e \rightarrow \nu_a$ transition model without any sterile neutrino, which would not be the case for the two parameter fit .⁶

A comparison of Figs. 2 and 3 shows the enormous improvement in precision one expects by including the NC rate from SNO . The vertical lines indicate the 2σ limits on f_B from the SSM . Combining the two limits one could rule out models having $\sin^2 \alpha < 0.3$ (i.e. singlet neutrino component $\cos^2 \alpha > 0.7$) at 2σ level for $R_{SNO}^{NC} = 0.8 \pm .08$, while $R_{SNO}^{NC} = 1.2 \pm .08$ would rule out all those singlet neutrino models with $\sin^2 \alpha < 0.6$ ($\cos^2 \alpha > 0.4$). However within the present uncertainty of the SSM value of the 8B neutrino flux it is unlikely to rule out models with a ν_s component $\cos^2 \alpha < 0.3$. Nor is it likely to set any upper limit on $\sin^2 \alpha$, which would show incompatibility with pure $\nu_e \rightarrow \nu_a$ transition.

Analysis of pure $\nu_e \rightarrow \nu_a$ Transition: Assuming no sterile neutrino the eqs. (6) and (8) reduce to

$$R_{SK}^{el} = f_B P_{ee} + f_B r(1 - P_{ee}), \quad (16)$$

$$R_{SNO}^{NC} = f_B. \quad (17)$$

In this case it is possible to estimate both f_B and P_{ee} from the SK elastic and the SNO CC rates even without the NC rate from SNO .⁷ Fig. 4 shows the 1 and 2 sigma contours of this solution along with the corresponding ones obtained by including the R_{SNO}^{NC} input. Our result in the former case is in good agreement with that of ref. ⁷, although the two methods are not identical. Thanks to the effective energy independence of the survival probability the result is insensitive to the difference between the energy thresholds of the SK elastic and the SNO CC rates. Unfortunately the resulting f_B has large error, which reflects the low sensitivity of R_{SK}^{el} to f_B (eq. 16). Interestingly both the central value and the error bar of f_B are practically the same as those of the SSM (shown for comparison near the right scale). The error in f_B propagates into P_{ee} due to a strong anticorrelation between the two quantities as their product is well constrained by R_{SNO}^{CC} (7). Fig. 4 shows that the inclusion of the NC rate from SNO will result in a reduction in the uncertainty of the 8B neutrino flux f_B and the corresponding survival probability P_{ee} by about a factor of 2.5.

The $\nu_e \rightarrow \nu_a$ oscillation solutions to the Solar Neutrino Anomaly: Finally we shall fit the global solar neutrino data with a standard two-family ($\nu_e \rightarrow \nu_a$) oscillation model assuming the SSM fluxes, but with one difference. Instead of R_{SK}^{el} and R_{SNO}^{CC} we shall fit the ratios R_{SK}^{el}/R_{SNO}^{NC} and $R_{SNO}^{CC}/R_{SNO}^{NC}$. As we see from eqs. (7,16,17) the 8B neutrino flux f_B factors out from these two ratios. Thus the result becomes immune to the large uncertainty in the SSM value of the 8B neutrino flux (5). We shall include the 19 + 19 day-night spectral points from SK , but with free normalisation to avoid double counting .^{7,8,10} We shall also include

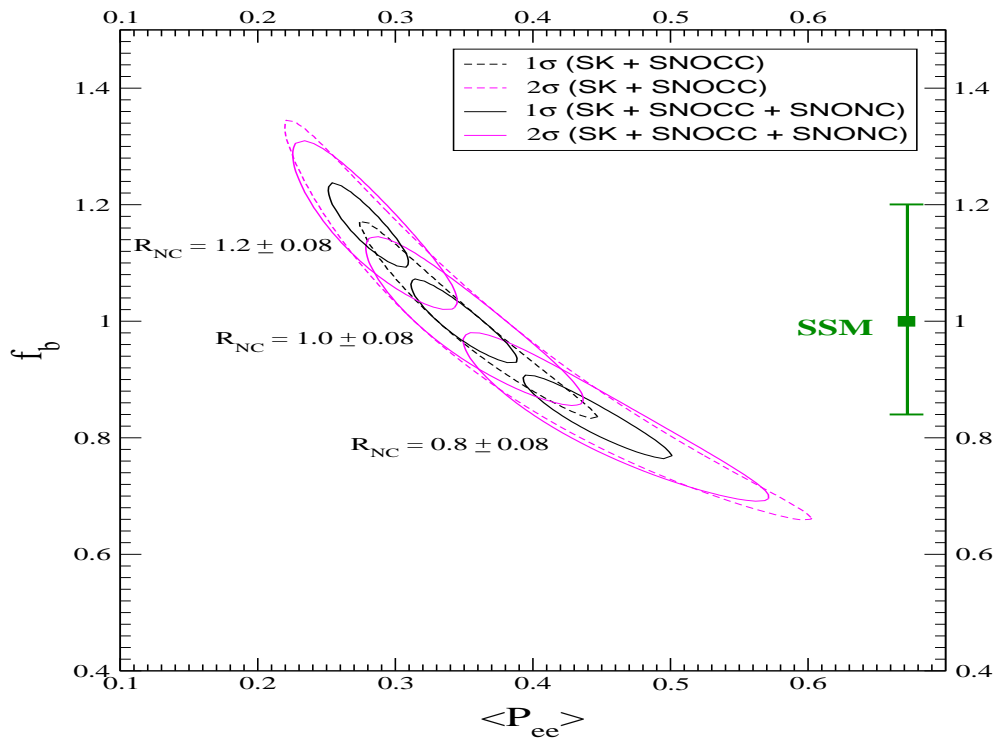


Fig. 4. The 1 and 2σ contours of solutions to the 8B neutrino flux f_B and the ν_e survival probability P_{ee} assuming ν_e to ν_a transition. The size of the *SSM* error bar for f_B is indicated on the right.

the combined Ga rate of Table 1 in the fit. However we shall exclude the Cl rate, since the experiment has not been independently calibrated. Besides the apparent rise of the CC rate between the Cl and SK/SNO energies is in conflict with the LMA and LOW solutions, which are strongly favoured by the global fit.¹⁰ Fig. 5 shows the 90%, 95%, 99% and 99.73% (3σ) CL contours of the fits for the three representative values of R_{SNO}^{NC} (10), which is the same as f_B (eq. 17). We have checked that all the three fits have equally good χ_{\min}^2 (~ 30) and goodness of fit ($\sim 80\%$).

The left panel of Fig. 5 represents $R_{SNO}^{SNC} = f_B = 0.8 \pm .08$. It corresponds to enhancing the survival probability P_{ee} at SK/SNO from 0.35 to nearly 0.45, while P_{ee} at Ga energy goes up by only 2%. Thus the energy dependence of P_{ee} between the Ga and SK/SNO energies become very mild. Consequently the solution favours large mixing angle, going upto maximal mixing, where it remains valid over two large mass ranges around $\delta m^2 = 10^{-4} \text{ eV}^2$ and 10^{-7} eV^2 .¹¹ These are the so called LMA and LOW solutions. In the present context however it will be more appropriate to call them $HIGH$ and LOW solutions, since both of them correspond to large mixing angles. The middle panel represents $R_{SNO}^{NC} = f_B = 1.0 \pm .08$, which means that the survival probability P_{ee} at Ga and SK/SNO energies corresponds to those shown in Table 1. Since such a large energy dependence cannot be explained by the earth matter effect, the LOW solution is only allowed at the 3σ level. On the other hand the $HIGH$ solution occurs at the upper edge of the MSW region in $\delta m^2/E$. Thus the survival probability goes down from $P_{ee} \simeq 1 - \frac{1}{2} \sin^2 2\theta > 0.5$ above the MSW region to $P_{ee} \simeq \sin^2 \theta$ inside it as one moves up from Ga to SK/SNO energies.¹⁰ The right panel corresponds to $R_{SNO}^{NC} = f_B = 1.2 \pm .08$, which means that the survival probability at SK/SNO energies goes down further by a factor of 1.2. Consequently the LOW solution disappears completely while the $HIGH$ solution moves to a lower mixing angle. Thus the measured value of the NC rate at SNO can have a profound effect on the mass and mixing angle of the solar neutrino oscillation solution.

Summary:

In anticipation of the first NC rate from SNO we have analysed how this data will sharpen our understanding of the solar neutrino anomaly. For a quantitative analysis we have chosen three representative value of this rate, $R_{SNO}^{NC} = 0.8, 1.0$ and $1.2(\pm .08)$. They span the $\pm 1\sigma$ range of this quantity as estimated from the SK elastic and SNO CC rates. The main results are listed below.

- (i) It will provide a $5 - 10\sigma$ signal for ν_e transition into an active flavor ν_a (or against a pure ν_e transition into a sterile neutrino ν_s).
- (ii) However for transition into a mixture of ν_a and ν_s , we need to know the 8B neutrino flux to constrain the size of the sterile component. If we assume the SSM prediction for this flux then $R_{SNO}^{NC} = 1.2 \pm .08$ ($0.8 \pm .08$) would imply the sterile component to be $< 40\%$ (70%) at the 2σ level.

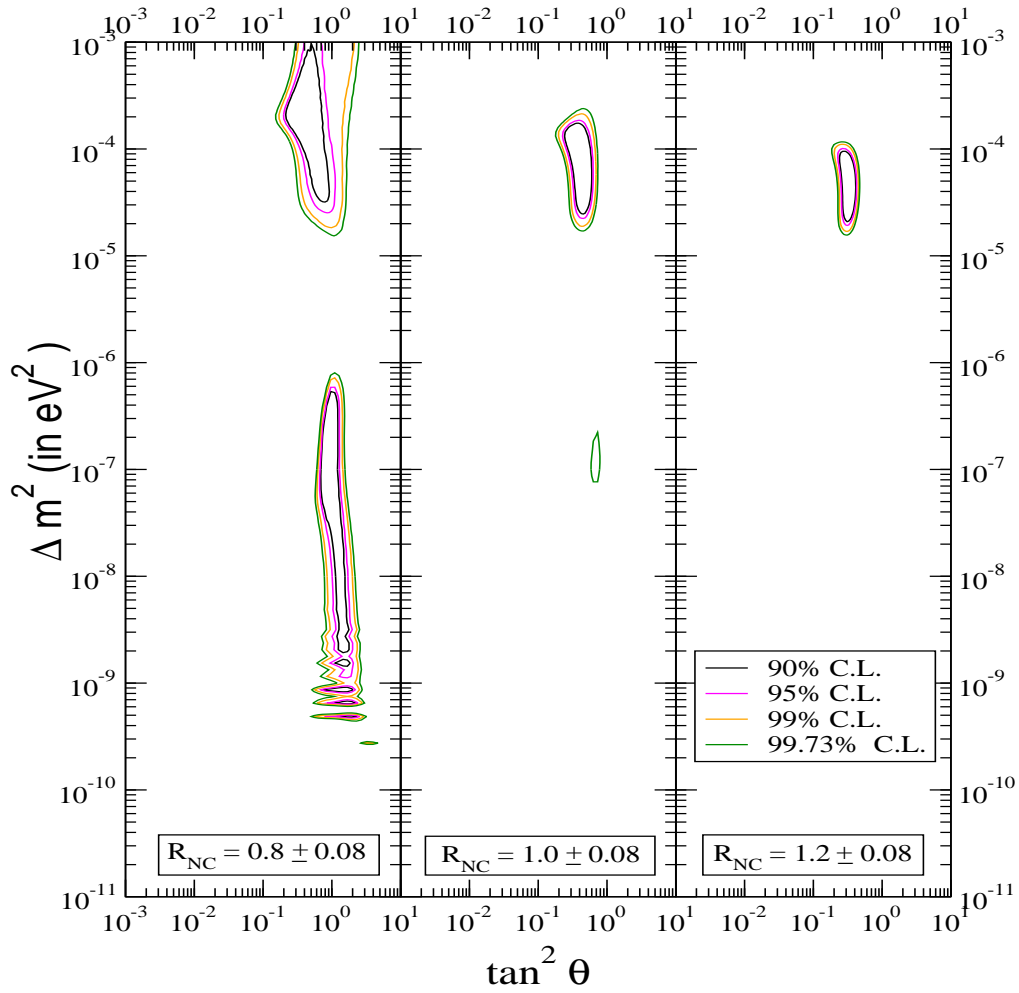


Fig. 5. The $\nu_e \rightarrow \nu_a$ oscillation solutions to the *Ga* rate, *SK* day-night energy spectra along with the *SK* and *SNO* (*CC*) rates, both normalised by the *SNO* (*NC*) rate.

- (iii) Assuming a pure $\nu_e \rightarrow \nu_a$ transition one can combine R_{SNO}^{NC} with R_{SNO}^{CC} and R_{SK}^{el} to determine both the 8B neutrino flux and the ν_e survival probability to much higher precision than is possible now from the latter two data.
- (iv) Finally one can do a $\nu_e \rightarrow \nu_a$ oscillation model fit to the global solar neutrino data assuming the *SSM* fluxes, but replacing the R_{SK}^{el} and R_{SNO}^{CC} by the ratios R_{SK}^{el}/R_{SNO}^{NC} and $R_{SNO}^{CC}/R_{SNO}^{NC}$, which are independent of the 8B neutrino flux. For $R_{SNO}^{NC} = 0.8 \pm .08$ we get both the *LMA (HIGH)* and *LOW* solutions covering large ranges of mass and mixing angle, including maximal mixing. On the other hand $R_{SNO}^{NC} \geq 1$ strongly disfavours the *LOW* solution, while the *HIGH* solution is restricted to a small patch in mass and mixing angle excluding maximal mixing. Thus the measured value of R_{SNO}^{NC} can have a profound effect on the mass and mixing parameters of the solar neutrino oscillation.

Acknowledgments

We thank S. Umasankar for discussions.

References

1. GNO Collaboration: M. Altmann *et al.*, *Phys. Lett.* **B490**, 16 (2000); Gallex Collaboration: W. Hampel *et al.*, *Phys. Lett.* **B447** (1999); SAGE Collaboration: J.N. Abdurashitov *et al.*, *Phys. Rev.* **C60**, 05580 (1999).
2. B.T. Cleveland *et al.*, *Astrophys. J.* **496**, 505 (1998).
3. S.K. Collaboration: S. Fukuda *et al.*, hep-ex/0103032.
4. SNO Collaboration: Q.R. Ahmad *et al.*, *Phys. Rev. Lett.* **87**, 071301 (2001).
5. J.N. Bahcall, M.H. Pinsonneault and S. Basu, *Astrophys. J.* **555**, 990 (2001).
6. V. Barger, D. Marfatia and K. Whisnant, *Phys. Rev. Lett.* **88**, 011302 (2002).
7. G.L. Fogli, E. Lisi, D. Montanino and A. Palazzo, *Phys. Rev.* **D64**, 093007 (2001).
8. A. Bandyopadhyay, S. Choubey, S. Goswami and K. Kar, *Phys. Lett.* **B519**, 83 (2001); S. Choubey, S. Goswami and D.P. Roy, *Phys. Rev.* **D65**, 073001(2002); A. Bandyopadhyay, S. Choubey, S. Goswami and K. Kar, hep-ph/0110307(to be published in *Phys. Rev. D*); P. I. Krastev and A. Y. Smirnov, hep-ph/0108117; S. Choubey, S. Goswami, K. Kar, H.M. Antia and S.M. Chitre, *Phys. Rev.* **D64**,113001(2001).
9. J.N. Bahcall, M.C. Gonzalez-Garcia and C. Pena-Garay, *JHEP* **0108**, 014 (2001); J.N. Bahcall, M.C. Gonzalez-Garcia and C. Pena-Garay, hep-ph/0111150.
10. C. Giunti, *Phys. Rev.***D65**, 033006(2002).
11. S. Choubey, S. Goswami, N. Gupta and D.P. Roy, *Phys. Rev.***D64**, 053002 (2001).